Tuning Metal-to-Metal Charge Transfer of Mixed-Valence Complexes Containing Ferrocenylpyridine and Rutheniumammines via Solvent Donicity and Substituent Effects

Yuan Jang Chen, Ching-Hong Kao, She Jing Lin, Chih-Cheng Tai, and Keh Shin Kwan*

Department of Chemistry, Fu Jen University, Taipei, Taiwan, Republic of China

Received July 15, 1999

A homogeneous series of heterobimetallic complexes of [R-Fc(4-py)Ru$(NH_3)_5$]$(PF_6)_2$ (R = H, Et, Br, acetyl; Fc(4-py) = 4-ferrocenylpyridine) have been prepared and characterized. The mixed-valence species generated in situ using ferrocenium hexafluorophosphate as the oxidant show class II behavior, and the oxidized sites are ruthenium centered. $\Delta E_{1/2}$, $E_{1/2}(Fe^{III}/Fe^{II}) - E_{1/2}(Ru^{III}/Ru^{II})$, an upper limit for $\Delta G°$ that is an energetic difference between the donor and acceptor sites, changes sharply and linearly with Gutmann solvent donor number (DN) and Hammett substituent constants (σ). The solvent-dependent and substituent-dependent intervalence transfer bands were found to vary almost exclusively with $\Delta E_{1/2}$. The activation energy for the optical electron transfer versus $\Delta E_{1/2}$ plot yields a common nuclear reorganization energy (λ) of 0.74 ± 0.04 eV for this series. The equation that allows one to incorporate the effect of both solvent donicity and substituents on optical electron transfer is $E_{op} = \lambda + \Delta G°$, where $\Delta G° = (\Delta G°)_{intrinsic} + (\Delta G°)_{solvent\ donicity} + (\Delta G°)_{substituent\ effect}$. $(\Delta G°)_{intrinsic}$ with a numerical value of 0.083 ± 0.045 eV was obtained from the intercept of the $\Delta E_{1/2}$ of [H-Fc(4-py)Ru$(NH_3)_5]^{2+,3+,4+}$ versus DN plot. $(\Delta G°)_{solvent\ donicity}$ was obtained from the average slopes of the $\Delta E_{1/2}$ of [R-Fc(4-py)Ru$(NH_3)_5]^{2+,3+,4+}$ versus DN plot, and $(\Delta G°)_{substituent\ effect}$ was obtained from the average slopes of the corresponding $\Delta E_{1/2}$ versus σ plot. The empirical equation allows one to finely tune E_{op} of this series to $E_{op} = 0.82 + 0.019(DN) + 0.44\sigma$ eV at 298 K, and the discrepancy between the calculated and experimental data is less than 6%.

Introduction

A potential energy description of optical and thermal electron transfer of an endothermic electron-transfer reaction can be depicted as

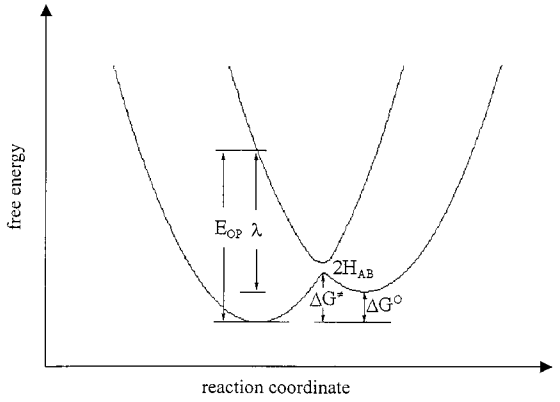

where E_{op} is the energy required for optical electron-transfer, λ is the nuclear reorganization energy, $\Delta G^{‡}$ is the activation barrier for thermal electron-transfer, H_{AB} is the electronic coupling matrix between the potential energy surfaces of reactants and products, and $\Delta G°$ is the free energy difference between products and reactants. According to Marcus−Hush theory,[1−8] these parameters of the optical and thermal electron-transfer process are closely interrelated by the relevant equations

$$E_{op} = \lambda + \Delta G° \quad (1)$$

$$\Delta G^{‡} = (\lambda + \Delta G°)^2/4\lambda \quad (2)$$

where λ is the algebraic sum of λ_i, the inner-sphere reorganization energy, and λ_o, the outer-sphere reorganization energy

$$\lambda = \lambda_i + \lambda_o \quad (3)$$

$$\lambda_0 = e^2\left(\frac{1}{2a_1} + \frac{1}{2a_2} - \frac{1}{r}\right)\left(\frac{1}{\epsilon_{op}} - \frac{1}{\epsilon_s}\right) \quad (4)$$

where e is the electronic charge transferred, a_1 and a_2 are the radii of spherical donor and acceptor sites whose metal−metal separation is r, and ϵ_{op} and ϵ_s are the optical and static dielectric constants of the medium, respectively. The electronic coupling matrix H_{AB} can be calculated by the expression

$$H_{AB} = (2.05 \times 10^{-2})\left[\frac{\epsilon_{max}\Delta\nu_{1/2}}{\nu_{max}}\right]^{1/2}\frac{\nu_{max}}{\gamma}\ \ cm^{-1} \quad (5)$$

$$\Delta\nu_{1/2} = [16(\ln 2)k_bT\lambda]^{1/2} \quad (6)$$

where $\Delta\nu_{1/2}$ is the half-bandwidth at the IT (intervalence transfer) band maximum (cm^{-1}), ν_{max} is the IT band maximum (cm^{-1}), ϵ_{max} is the molar absorptivity ($M^{-1}cm^{-1}$) at the band maximum, and r is the intermetallic separation (Å).

(1) Marcus, R. A. *J. Chem. Phys.* **1956**, *24*, 966.
(2) Marcus, R. A. *Annu. Rev. Phys. Chem.* **1964**, *15*, 155.
(3) Marcus, R. A.; Sutin, N. *Biochim. Biophys. Acta* **1985**, *811*, 265.
(4) Marcus, R. A.; Siders, P. *J. Phys. Chem.* **1982**, *86*, 622.
(5) Marcus, R. A.; Sutin, N. *Inorg. Chem.* **1975**, *14*, 213.
(6) Sutin, N. *J. Photochem.* **1979**, *10*, 19.
(7) Hush, N. S. *Prog. Inorg. Chem.* **1967**, *8*, 391.
(8) Hush, N. S. *Coord. Chem. Rev.* **1985**, *64*, 135.

10.1021/ic990839j CCC: $19.00
Published on Web 01/04/2000

Table 1. $E_{1/2}$ Values and Comproportionation Constants of [R-Fc(4-Py)Ru(NH_3)$_5$](PF_6)$_2$ (R = Et, H, Br, Acetyl) in Various Solvents[a]

		[Et-Fc(4-Py)Ru(NH_3)$_5$]$^{3+}$				[H-Fc(4-Py)Ru(NH_3)$_5$]$^{3+}$				[Br-Fc(4-Py)Ru(NH_3)$_5$]$^{3+}$				[Ac-Fc(4-Py)Ru(NH_3)$_5$]$^{3+}$			
solvent	DN[b]	$(E_{1/2})_1$	$(E_{1/2})_2$	$\Delta E_{1/2}$	K_c[c]	$(E_{1/2})_1$	$(E_{1/2})_2$	$\Delta E_{1/2}$	K_c[c]	$(E_{1/2})_1$	$(E_{1/2})_2$	$\Delta E_{1/2}$	K_c[c]	$(E_{1/2})_1$	$(E_{1/2})_2$	$\Delta E_{1/2}$	K_c[c]
DMSO	29.8	−510	130	640	6.6×10^{10}	−491	208	699	6.6×10^{11}	−490	324	814	5.8×10^{13}	−482	434	916	3.1×10^{15}
DMA	27.8	−447	193	640	6.6×10^{10}	−431	271	702	7.4×10^{11}	−414	408	822	7.9×10^{13}	−412	*e*	*f*	
DMF	26.6	−421	182	603	1.6×10^{10}	−409	254	663	1.6×10^{11}	−403	379	782	1.7×10^{13}	−397	459	856	3.0×10^{14}
C_2H_5OH	20	−67	273	340	5.6×10^{5}	−65	336	401	6.0×10^{6}			*f*				*f*	
CH_3OH	19	−101	261	362	1.3×10^{6}	−95	321	416	1.1×10^{7}	−65	493	558	2.7×10^{9}	−60	560	620	3.0×10^{10}
CH_3COCH_3	17	−145	236	381	2.8×10^{6}	−135	297	432	2.0×10^{7}	−113	456	569	4.2×10^{9}	−110	531	641	6.9×10^{10}
PC[d]	15.1	−157	186	343	6.3×10^{5}	−141	254	395	4.8×10^{6}	−123	404	527	8.1×10^{8}	−119	499	618	2.9×10^{10}
CH_3CN	14.1	−62	235	297	1.0×10^{5}	−39	305	344	6.5×10^{5}	−28	447	475	1.1×10^{8}	−23	533	556	2.5×10^{9}
benzonitrile	11.9	0	290	290	8.0×10^{4}	30	365	335	4.6×10^{5}	32	510	478	1.2×10^{8}	40	590	550	2.0×10^{9}
nitrobenzene	4.4	110	280	170	7.5×10^{2}	134	248	214	4.1×10^{3}	140	500	360	1.2×10^{6}	150	610	460	6.0×10^{7}
nitromethane	2.7	90	220	130	1.6×10^{2}	110	260	150	3.4×10^{2}	112	432	320	2.6×10^{5}	120	525	405	7.0×10^{6}

[a] Data are in mV. The values of $E_{1/2}$ were measured against the a PAR-KO103 nonaqueous reference electrode, Ag/0.1 M $AgNO_3$ in CH_3CN, located inside a reference electrode bridge tube with a Vycor tip (PAR−K0065). These values are the average of the potentials for peak anodic and cathodic currents in the cyclic voltammograms recorded at 200 mV/s. $\Delta E_{1/2}$ ($\Delta E_{1/2} = E_{1/2}(Fe^{III}/Fe^{II}) - E_{1/2}(Ru^{III}/Ru^{II})$). [b] Taken from ref 12. [c] Calculated from eqs 7 and 8. [d] Propanediol-(1,2)-carbonate. [e] Ferrocene peak not observed. [f] Not observed due to poor solubility.

The effect of solvent on optical and thermal electron-transfer of class II mixed-valence complexes[9] through λ can be clearly seen from eqs 1−4. Equally important whereas not so obvious is the effect of solvent on the intervalence transitions by changing $\Delta G°$. Lay,[10] Curtis,[11] and others[12−15] have elucidated the linear relationship between $\Delta G°$ and the Gutmann solvent donor number.[16] The effect of preferential solvation and solvent−solute interactions of unsymmetrical mixed-valence complexes are important issues and bear current interests in electron-transfer research.[17−24] To extend our work and to understand the effect upon the electrochemical and near-infrared properties by changing substituents on the Cp ring, a homogeneous series of mixed-valence compounds

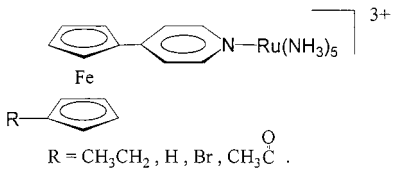

where R = Et, H, Br, and acetyl were synthesized. In the course to elucidate the degree of electronic interaction between metal centers in these systems, we uncover a good linear relationship among E_{op}, λ, solvent donicity, and substituent effects so as to make tuning IT predictable.

Results and Discussion

Electrochemistry. The cyclic voltammograms of the four heterobimetallic complexes in all solvents studied display two reversible metal-based redox couples, and the electrochemical data are given in Table 1. The first oxidation in each case corresponds to oxidation of Ru(II)/Ru(III), and the second oxidation corresponds to Fe(II)/Fe(III). These assignments were made by analogy to the R−Fc(4-py) moieties and previously reported mono- and bimetallic systems.[14,25] The presence of two one-electron oxidations, instead of one two-electron oxidation, indicates a stabilization of the mixed-valence species. The separation between the two oxidation potentials, $\Delta E_{1/2}$ ($\Delta E_{1/2} = E_{1/2}(Fe^{III}/Fe^{II}) - E_{1/2}(Ru^{III}/Ru^{II})$), was employed to calculate the comproportionation constant, K_c, from the following equations:

$$(Ru^{II}, Fe^{II}) + (Ru^{III}, Fe^{III}) \rightleftharpoons 2(Fe^{II}, Ru^{III}) \qquad K_c \quad (7)$$

$$\Delta E_{1/2}\ (\text{mV}) = 59.15(\log K_c) \qquad \text{at 298 K} \qquad (8)$$

As can be seen in Table 1, values of K_c of each complex vary by 8 orders of magnitude due to the solvent donicity[16] and 4 orders of magnitude due to substituent effects. They range from 1.6×10^2 in the smallest donor number solvent CH_3NO_2 with an electron-donating ethyl group to 3×10^{15} in the largest donor number solvent DMSO with an electron-withdrawing acetyl group. These results indicate that the electronic coupling between metal centers can be finely tuned by way of choosing the appropriate solvent and the substituent group.

UV−Vis Spectra. The electronic spectra of R−Fc(4-py) and [R-Fc(4-py)Ru(NH_3)$_5$]$^{n+}$ (R = H, Et, Br, acetyl; n = 2, 3) are summarized in Table 2. The UV absorption bands between 200 and 300 nm for R-Fc(4-py) were assigned to Fe(dπ) → Cp(π*) charge transfer or $\pi \rightarrow \pi$* transitions, or additive contributions of these transitions. The longer wavelength bands between 330 and 466 nm were assigned to d−d transitions within the ligand field formalism. These assignments are consistent with the

(9) Robin, M. B.; Day, P. Adv. *Inorg. Chem.* **1967**, *10*, 247.
(10) Lay, P. A. *J. Phys. Chem.* **1986**, *90*, 878.
(11) (a) Chang, J. P.; Fung, E. Y.; Curtis, J. C. *Inorg. Chem.* **1986**, *25*, 4233. (b) Ennix, K. S.; McMahon, P. T.; Rosa, R.; Curtis, J. C. *Inorg. Chem.* **1987**, *26*, 2660. (c) Fung, E. Y.; Chua, A. C. M.; Curtis, J. C. *Inorg. Chem.* **1988**, *27*, 1294. (d) Salaymeh, F.; Berhane, S.; Yusof, R.; Rosa, R.; Fung, E. Y.; Matamoros, R.; Lau, K. W.; Zheng, Q.; Kober, E. M.; Curtis, J. C. *Inorg. Chem.* **1993**, *32*, 3895. (e) Lau, K. W.; Hu, A. M.-H.; Yen, M. H.-J.; Fung, E. Y.; Grzybicki, S.; Matamoros, R.; Curtis, J. C. *Inorg. Chim. Acta* **1994**, *226*, 137. (f) Mao, W.; Qian, Z.; Yen, H.-J.; Curtis, J. C. *J. Am. Chem. Soc.* **1996**, *118*, 3247.
(12) Hupp, J. P. *J. Am. Chem. Soc.* **1990**, *112*, 1563.
(13) Wu, Y.; Cohran, C.; Bocarsly, A. B.*Inorg. Chim. Acta* **1994**, *226*, 251.
(14) Liu, T.-Y.; Chen, Y. J.; Tai, C.-C.; Kwan, K. S. *Inorg. Chem.* **1999**, *38*, 674.
(15) Pfennig, B. W.; Cohen, J. L.; Sosnowski, I.; Novotny, N. M.; Ho, D. M. *Inorg.* Chem. **1999**, *38*, 606.
(16) Gutmann, V. *The Donor-Acceptor Approach to Molecular Interactions*; Plenum: New York, 1978.
(17) Hush, N. S.; Reimers, J. R.*Coord. Chem. Rev.* **1998**, *177*, 37.
(18) Barbara, P. F.; Meyer, T. J.; Ratner, M. A. *J. Phys. Chem.* **1996**, *100*, 13148.
(19) (a) Drago, R. S.; Ferris, D. C. *J. Phys. Chem.* **1995**, *99*, 6563. (b) Drago, R. S.; Richardson, D. E.; George, J. E. *Inorg. Chem.* **1997**, *36*, 25.
(20) Sauvage, J.-P.; Collin, J.-P.; Chambron, J.-C.; Guillerez, S.; Coudret, C. *Chem. Rev.* **1994**, *94*, 993.
(21) Weaver, M. J.*Chem. Rev.* **1992**, *92*, 463.
(22) Barbara, P. F.; Walker, G. C.; Smith, T. P. *Science* **1992**, *256*, 975.
(23) Heitele, H. *Angew. Chem., Int. Ed. Engl.* **1993**, *32*, 359.
(24) Yoshihara, K.; Tominaga, K.; Nagasawa, Y. *Bull. Chem. Soc. Jpn.* **1995**, *68*, 696.
(25) Lavallee, D. K.; Fleischer, E. B. *J. Am. Chem. Soc.* **1972**, *94*, 2583.

Table 2. Electronic Spectra of $[R\text{-}Fc(4\text{-}Py)Ru(NH_3)_5]^{3+}$ (R = Ethyl, H, Bromo, Acetyl)[a]

complex	λ_{max}	$10^{-3}\epsilon_{max}$	complex	λ_{max}	$10^{-3}\epsilon_{max}$
Fc(4-Py)	242	11.37	Br−Fc(4-Py)	243	14.4
	280	8.26		281	9.92
	342	1.30		331	1.40
	466	0.38		449	0.48
$[Fc(4\text{-}Py)Ru(NH_3)_5]^{2+}$	248	14.8	$[Br-Fc(4\text{-}Py)Ru(NH_3)_5]^{2+}$	245	17.2
	280	10.8		282[b]	10.0
	438	12.6		431	9.86
$[Fc(4\text{-}Py)Ru(NH_3)_5]^{3+}$	250	12.5	$[Br-Fc(4\text{-}Py)Ru(NH_3)_5]^{3+}$	246	14.0
	385	13.8		282[b]	11.7
	396	3.32		369	3.64
	1092	0.61		993	0.55
Et-Fc(4-Py)	245	13.7	Ac−Fc(4-Py)	237	18.0
	278	12.4		265	16.0
	344	1.58		333	2.34
	453	0.54		458	0.66
$[Et\text{-}Fc(4\text{-}Py)Ru(NH_3)_5]^{2+}$	250	13.8	$[Ac-Fc(4\text{-}Py)Ru(NH_3)_5]^{2+}$	223	28.1
	281	9.48		273	48.8
	433	11.8		440	9.62
$[Et\text{-}Fc(4\text{-}Py)Ru(NH_3)_5]^{3+}$	240	15.2	$[Ac-Fc(4\text{-}Py)Ru(NH_3)_5]^{3+}$	242	15.3
	280	12.0		284[b]	11.6
	396	3.20		378	3.6
	1166	0.78		938	0.47

[a] Spectra taken in CH_3CN, λ_{max} in nm, and ϵ_{max} in M^{-1} cm^{-1}. [b] Shoulder.

extensively discussed spectra of ferrocene.[26] When R-Fc(4-py) was coordinated to $Ru^{II}(NH_3)_5$, the mentioned longer wavelength and lower intensity bands were masked by a strong absorption band around 435 nm. On the basis of previously reported metal-to-ligand charge-transfer (MLCT) spectra of pentaammineruthenium(II) complexes of pyridine and other nitrogen heterocycles,[27−30] these were assigned to Ru^{II} ($d\pi$) to 4-py (π^*) charge transfer. The disappearance of these bands in $[R\text{-}Fc(4\text{-}py)Ru(NH_3)_5]^{3+}$ spectra further confirms that these bands are metal-to-ligand in nature, and that the oxidation is ruthenium centered.

Near-IR Spectra. Near-IR spectra in various solvents of $[R\text{-}Fc(4\text{-}py)Ru(NH_3)_5]^{3+}$ (R = H, Et, Br, acetyl) were measured. These spectra were compared to those of unoxidized (Fe^{II}, Ru^{II}) and fully oxidized (Fe^{III}, Ru^{III}) samples of the same concentration so that the intensity changes are relevant. As can be seen in Table 1, $(E_{1/2})_1$ values that correspond to redox potentials of $Ru^{II/III}$ have a span of 600 mV in various solvents for all four complexes. By contrast, $(E_{1/2})_2$ values that correspond to $Fe^{II/III}$ redox potentials of ferrocenyl moieties have a range of 150 mV or less in the corresponding cases. In Figure 1, we have plotted $\Delta E_{1/2}$ ($\Delta E_{1/2} = E_{1/2}(Fe^{III}/Fe^{II}) - E_{1/2}(Ru^{III}/Ru^{II})$) versus solvent donor number (DN).[16] Linear relationships were observed in all four complexes. For $[R\text{-}Fc(4\text{-}py)Ru(NH_3)_5]^{2+,3+,4+}$ where R = Et, we found a slope of 0.0192 ± 0.0016 V/DN, an intercept of 0.053 ± 0.047 V, and a correlation coefficient of 0.937. The corresponding values are 0.0204 ± 0.0016 V/DN, 0.083 ± 0.045 V, and 0.948 for R = H; 0.0192 ± 0.0012 V/DN, 0.248 ± 0.032 V, and 0.971 for R = Br; and 0.0182 ± 0.0015 V/DN, 0.340 ± 0.038 V, and 0.955 for R = acetyl, respectively. The consequence of Ru^{II} ($d\pi$) → π^* back-donation toward solvent donicity is clearly depicted in this figure where π back-donation is less extensive in low donor number solvents. Similar observations have been previously reported.[31,32] In Figure 2, we have plotted $\Delta E_{1/2}$ of $[R\text{-}Fc(4\text{-}py)Ru(NH_3)_5]^{2+,3+,4+}$ (R = Et, H, Br, acetyl) in each solvent versus Hammett substituent constants (σ).[27] A linear relationship was observed in each case with a slope in the order 0.46 ± 0.01, 0.46 ± 0.02, 0.42 ± 0.02, 0.45 ± 0.03, 0.44 ± 0.04, 0.47 ± 0.02, 0.44 ± 0.02, 0.45 ± 0.03, and 0.49 ± 0.05 V/σ for DMSO, DMA, DMF, acetone, CH_3OH, propanediol-(1,2)-carbonate (PC), acetonitrile, benzonitrile, nitrobenzene, and CH_3NO_2, respectively. These lines are essentially parallel with an average value of 0.44 ± 0.04 V/σ, indicating substituent effects to be independent of solvation and Hammett substituent constants to be applicable in the Cp

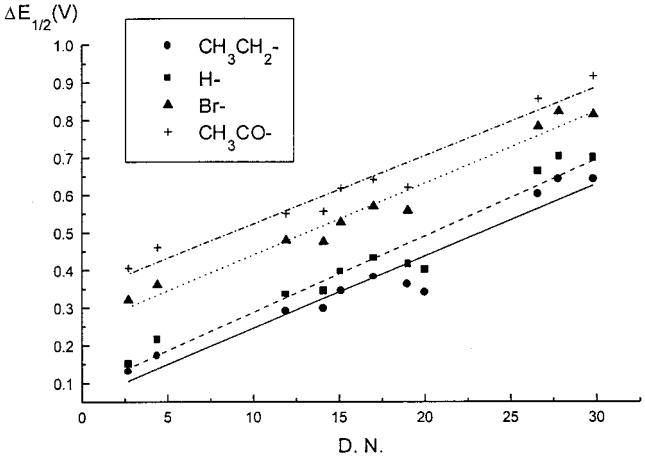

Figure 1. $\Delta E_{1/2}$ ($E_{1/2}(Fe^{III}/Fe^{II}) - E_{1/2}(Ru^{III}/Ru^{II})$) versus Gutmann solvent donor number (DN) for $[R\text{-}Fc(4\text{-}py)Ru(NH_3)_5]^{3+}$.

(26) (a) Scott, D. R.; Becker, R. S. *J. Chem. Phys.* **1962**, *35*, 516. (b) Scott, D. R.; Becker, R. S. *J. Chem. Phys.* **1962**, *35*, 2246.
(27) Ford, P.; Rudd, D. F. P.; Gaunder, R.; Taube, H. *J. Am. Chem. Soc.* **1968**, *90*, 1187.
(28) Rieder, K.; Taube, H. *J. Am. Chem. Soc.* **1977**, *99*, 7891.
(29) Fisher, M.; Tom, G. M.; Taube, H. *J. Am. Chem. Soc.* **1976**, *98*, 5512.
(30) Richardson, D. E.; Taube, H. *J. Am. Chem. Soc.* **1983**, *105*, 40.
(31) Chang, J. P.; Fung, E. Y.; Curtis, J. C. *Inorg. Chem.* **1986**, *25*, 4233.
(32) Creutz, C.; Chou, M. H. *Inorg. Chem.* **1987**, *26*, 2995.
(33) Muroy, S. L.; Carmichael, I.; Hug, G. L. *Handbook of Photochemistry*; Marcel Dekker: New York, 1993.

Table 3. Data for Intervalence Transfer Bands of $[R\text{-}Fc(4\text{-}py)Ru(NH_3)_5]^{3+}$ in Various Solvents

	$[Et\text{-}Fc(4\text{-}Py)Ru(NH_3)_5]^{3+}$					$[Fc(4\text{-}Py)Ru(NH_3)_5]^{3+}$					$[Br-Fc(4\text{-}Py)Ru(NH_3)_5]^{3+}$					$[Ac\text{-}Fc(4\text{-}Py)Ru(NH_3)_5]^{3+}$				
solvent	ν_{max}	ν_{calc}[b]	ϵ_{max}	$\Delta\nu_{1/2}$	H_{AB}	ν_{max}	ν_{calc}[b]	ϵ_{max}	$\Delta\nu_{1/2}$	H_{AB}	ν_{max}	ν_{calc}[b]	ϵ_{max}	$\Delta\nu_{1/2}$	H_{AB}	ν_{max}	ν_{calc}[b]	ϵ_{max}	$\Delta\nu_{1/2}$	H_{AB}
DMSO	1.39	1.32	440	507	46.2	1.45	1.39	380	455	41.6	1.54	1.49	275	487	37.8	1.59	1.60	260	492	37.6
DMA	1.37	1.28	480	517	48.5	1.42	1.35	340	464	39.4	1.53	1.45	280	474	37.4	1.57	1.56	260	512	37.9
DMF	1.37	1.26	420	549	46.7	1.42	1.32	360	456	40.0	1.53	1.42	300	483	39.2	1.58	1.54	270	509	38.7
C_2H_5OH	1.12	1.13	670	506	51.2	1.19	1.20	590	452	46.9										
CH_3OH	1.15	1.11	640	502	50.5	1.20	1.18	550	454	45.5	1.33	1.28	490	472	46.1	1.36	1.40	400	475	42.3
CH_3COCH_3	1.16	1.07	680	496	51.9	1.21	1.14	560	455	46.2	1.34	1.24	510	457	46.4	1.39	1.36	450	491	46.1
PC	1.09	1.04	670	480	49.3	1.17	1.11	500	471	43.6	1.29	1.21	470	455	43.6	1.36	1.32	410	540	45.6
CH_3CN	1.06	1.02	780	473	52.1	1.14	1.09	610	470	47.4	1.25	1.19	550	457	46.5	1.32	1.30	470	502	46.4
benzonitrile	1.03	0.980	830	478	53.1	1.08	1.05	700	468	49.6	1.21	1.15	630	447	48.6	1.28	1.26	540	446	46.1
nitrobenzene	0.838	0.838	910	484	50.5	0.896	0.904	810	481	49.1	1.02	1.00	740	458	47.7	1.10	1.12	610	454	45.8
nitromethane	0.833	0.806	1020	523	55.4	0.862	0.871	880	496	51.0	1.02	0.973	800	477	51.9	1.08	1.09	680	488	49.7
substituent constant, σ	Et = −0.15					H = 0					Br = 0.23					Ac = 0.50				

[a] ν_{max} and ν_{calc} in eV, ϵ_{max} in M^{-1} cm^{-1}, $\Delta\nu_{1/2}$ and H_{AB} in meV. [b] ν_{calc} calculated from eq 8.

Table 4. Rate Constants and Activation Energies for Thermal Electron Transfer of $[R\text{-}Fc(4\text{-}py)Ru(NH_3)_5]^{3+}$ in Various Solvents[a]

	$[Et\text{-}Fc(4\text{-}Py)Ru(NH_3)_5]^{3+}$				$Fc(4\text{-}Py)Ru(NH_3)_5]^{3+}$				$[Br\text{-}Fc(4\text{-}Py)Ru(NH_3)_5]^{3+}$				$[Ac-Fc(4\text{-}Py)Ru(NH_3)_5]^{3+}$			
solvent	ν_{el}	κ	$\Delta G^{\ddagger}$	k_{th}, s^{-1}	ν_{el}	κ	$\Delta G^{\ddagger}$	k_{th}, s^{-1}	ν_{el}	κ	$\Delta G^{\ddagger}$	k_{th}, s^{-1}	ν_{el}	κ	$\Delta G^{\ddagger}$	k_{th}, s^{-1}
DMSO	42.3	0.993	596	4.18×10^2	33.9	0.983	658	3.76×10^1	28.5	0.970	780	3.23×10^{-1}	28.5	0.970	897	3.41×10^{-3}
DMA	46.5	0.995	594	4.56×10^2	30.3	0.975	663	3.07×10^1	27.9	0.968	789	2.27×10^{-1}	29.1	0.972		
DMF	43.2	0.993	561	1.64×10^3	31.3	0.978	625	1.36×10^2	30.6	0.976	745	1.28	30.2	0.975	827	5.14×10^{-2}
C_2H_5OH	51.9	0.997	339	9.31×10^6	42.9	0.993	393	1.14×10^6								
CH_3OH	50.4	0.997	356	5.50×10^6	40.4	0.991	406	6.83×10^5	42.4	0.993	520	8.06×10^3	36.1	0.986	580	7.94×10^2
CH_3COCH_3	53.4	0.998	369	2.88×10^6	41.8	0.992	418	4.32×10^5	42.9	0.993	530	5.56×10^3	43.0	0.980	596	4.22×10^2
PC	48.2	0.996	343	7.94×10^6	37.2	0.988	392	1.20×10^6	38.0	0.989	495	2.12×10^4	42.1	0.992	574	9.77×10^2
CH_3CN	53.7	0.998	307	3.22×10^7	43.8	0.994	350	6.12×10^6	43.1	0.993	448	1.33×10^5	43.4	0.993	516	9.40×10^3
benzonitrile	55.7	0.998	301	4.04×10^7	48.0	0.996	341	3.17×10^7	47.1	0.995	448	1.31×10^5	43.0	0.993	511	1.15×10^4
nitrobenzene	50.4	0.997	224	7.98×10^8	47.1	0.995	258	2.14×10^8	47.8	0.996	354	5.12×10^6	42.3	0.993	433	2.34×10^5
nitromethane	60.8	0.999	196	2.47×10^9	50.7	0.997	217	1.09×10^9	53.8	0.998	322	1.82×10^7	50.0	0.997	385	1.56×10^6

[a] ν_{el} in ps and $\Delta G^{\ddagger}$ in meV.

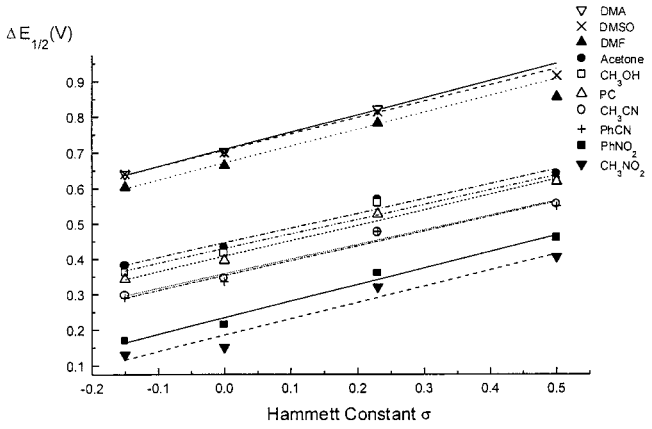

Figure 2. $\Delta E_{1/2}$ ($E_{1/2}(Fe^{III}/Fe^{II}) - E_{1/2}(Ru^{III}/Ru^{II})$) versus Hammett constants (σ) for $[R\text{-}Fc(4\text{-}py)Ru(NH_3)_5]^{3+}$.

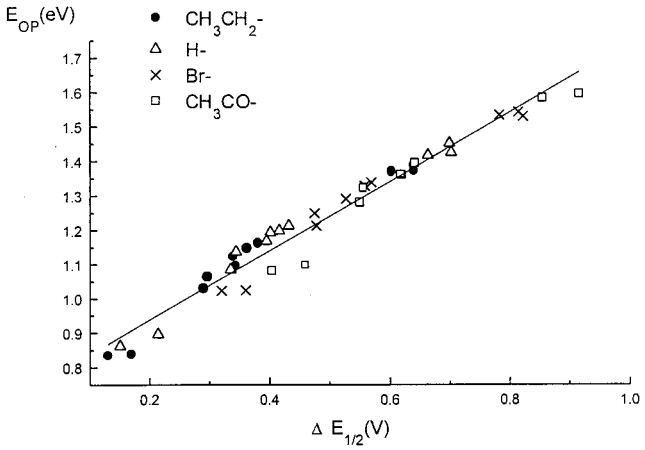

Figure 3. E_{op} versus $\Delta E_{1/2}$ ($E_{1/2}(Fe^{III}/Fe^{II}) - E_{1/2}(Ru^{III}/Ru^{II})$) for $[R\text{-}Fc(4\text{-}py)Ru(NH_3)_5]^{3+}$ with a slope of 1.01 ± 0.03 eV/V, an intercept of 0.74 ± 0.04 eV, and a correlation coefficient of 0.964.

ring system as well. Results of the IT band maximum ν_{max}, the molar absorptivity at the band maximum ϵ_{max}, the half-bandwidth at the IT band maximum $\Delta\nu_{1/2}$, and the metal−metal interaction parameter H_{AB} calculated from eq 5 are summarized in Table 3. In the calculation of H_{AB}, the intermetallic separation r was estimated to be 7.8 Å from crystallographic data[14] of Fc-(4-py) and a py−RuIII distance[30] of 2.0 Å. Figure 3 shows an E_{op} versus $\Delta E_{1/2}$ plot for $[R\text{-}Fc(4\text{-}py)Ru(NH_3)_5]^{3+}$ (R = H, Et, Br, acetyl) in all solvents studied. The least-squares fit of the straight line yields a slope of 1.01 ± 0.03 eV/V, an intercept of 0.74 ± 0.04 eV, and a correlation coefficient of 0.964. Our results indicate that the optical electron transfer in $[R\text{-}Fc(4\text{-}py)Ru(NH_3)_5]^{3+}$ is homogeneous with a common nuclear reorganization energy λ and that IT bands vary almost exclusively with $\Delta E_{1/2}$. To incorporate the effects of both solvent donicity and substituent on the optical electron transfer of this series, the intercept of the $\Delta E_{1/2}$ of $[H\text{-}Fc(4\text{-}py)Ru(NH_3)_5]^{2+,3+,4+}$ versus DN plot in Figure 2 is taken as the "intrinsic" $\Delta G°$. Then eq 8 transforms as

$$E_{op} = \lambda + (\Delta G°)_{intrinsic} + (\Delta G°)_{solvent\ donicity} + (\Delta G°)_{substituent\ effect} \doteq 0.82 + 0.019(DN) + 0.44\sigma \quad eV \quad (9)$$

Results calculated from eq 9 are also listed in Table 3. Considering $\Delta E_{1/2}$ values to be an upper limit[34] for $\Delta G°$, we

(34) Johnson, E. C.; Sullivan, B. P.; Salmon, D. J.; Adeyemi, S. A.; Meyer, T. J.*Inorg.* Chem. **1978**, *8*, 2211.

feel that the agreement between the calculated and experimental data are very satisfactory. The deviations in most cases are less than 5% with some scatter around 6%. Realizing the influence of the ionic association effect,[35,36] we chose all concentrations in this work to be as close to 1×10^{-3} M as possible and found the perturbation to be negligible.

It should be pointed out that the substituent and the solvent may also affect the degree of mixing (α) of the two states and hence the probability of electron transfer. If that is the case, the charge transferred will be decreased from e to $(1 - 2\alpha^2)e$, and λ_o will be decreased by $(1 - 2\alpha^2)e$ times as shown in eq 4.[37] However, the value of α^2 ranges from 5.6×10^{-4} to 3.6×10^{-3} for this series of mixed-valence complexes, which is apparently not large enough to perturb the observed linear relationship.

Conclusions

$[R\text{-}Fc(4\text{-}py)Ru(NH_3)_5]^{3+}$ (R = H, Et, Br, acetyl; Fc(4-py) = 4-ferrocenylpyridine) form a series of mixed-valence complexes with a constant nuclear reorganization energy. Their IT bands are solvent and substituent dependent and are found to vary almost exclusively with $\Delta E_{1/2}$, $E_{1/2}(Fe^{III}/Fe^{II}) - E_{1/2}(Ru^{III}/Ru^{II})$. Using $\Delta E_{1/2}$ as an estimate of $\Delta G°$ that is an energetic difference between the donor and acceptor sites, we found an empirical equation incorporating the Gutmann solvent donor number (DN) and Hammett substituent constants (σ) to finely tune E_{op} of this series within 94% accuracy.

Experimental Section

General Methods and Chemicals. All syntheses and manipulations were carried out using standard Schlenk techniques.[38] All yields reported refer to isolated material judged to be homogeneous by NMR spectroscopy. ^{1}H NMR spectra were obtained in $CDCl_3$ on a Bruker Aspect-3000 (300 MHz) spectrometer. All chemical shifts are in parts per million, relative to δ(tetramethylsilane) = 0 ppm. DMF and DMSO were dried over 4 Å molecular sieves, and benzonitrile was dried over $MgSO_4$. Acetone was dried over 4 Å molecular sieves and distilled to collect the fraction between 56 and 57 °C. Other solvents were dried according to an established procedure[39] by distillation under N_2 from appropriate drying agents: acetonitrile from CaH_2, nitrobenzene from P_2O_5, and DMA, methanol, and ethanol from CaO. Chemicals were obtained from the following sources: acetone-d_6 from MSD, Al_2O_3 from Fluka, and the rest from Aldrich.

Preparation of 1-Ethyl-1′-(4-pyridyl)ferrocene, [Et-Fc(4-py)]. Ethylferrocenylmagnesium bromide was prepared as described in the literature.[40] Acid-free 4-bromopyridine was obtained by neutralizing 4-bromopyridine hydrochloride with 1 M NaOH, and extracted with Et_2O. The ethereal solution was washed with saturated NaCl solution, dried over $MgSO_4$, and concentrated to a clear oil by rotary evaporation. A 100 mL three-necked flask containing 16.6 mg (31 μmol) of *cis*-(1,3-bis(diphenylphosphino)propane)−dichloronickel[41] and 0.41 g (2.6 mmol) of 4-bromopyridine in 10 mL of Et_2O was assembled with a magnetic stirring bar, condenser, and argon inlet and outlet. To this flask was slowly added ethylferrocenylmagnesium bromide prepared from 2.2 g (7.6 mmol) of 1-bromo-1′-ethylferrocene in 50 mL of Et_2O. The resulting mixture was stirred and refluxed overnight. The reaction was quenched by slow addition of 25 mL of H_2O, and the organic layer was collected, washed with brine, dried over $MgSO_4$, concentrated by rotary evaporation, and chromatographed on a silica gel column using a solution of 5% MeOH in ether. [Et-Fc(4-py)] was isolated in 80% yield as a red oil. Anal. Calcd for $C_{17}H_{17}NFe$: C, 70.13; H, 5.88; N, 4.81. Found: C, 69.90; H, 5.96; N, 4.76. ^{1}H NMR ($CDCl_3$): δ 8.46 (d, 2H), 7.29 (d, 2H), 4.64 (t, 2H), 4.35 (t, 2H), 3.90 (m, 4H), 2.10 (q, 2H), 1.03 (t, 3H). ^{13}C NMR ($CDCl_3$): δ 149.4, 120.3, 92.1, 80.6, 70.7, 69.2, 69, 67.1, 21.3, 14.6.

Preparation of 1-Acetyl-1′-(4-pyridyl)ferrocene, [Ac-Fc(4-py)]. This compound was obtained by oxidation of [Et-Fc(4-py)] with MnO_2. A 10 g sample of MnO_2 was added to a 100 mL CH_2Cl_2 solution containing 1 g (3.43 mmol) of [Et-Fc(4-py)] and stirred under argon overnight. After filtration, the CH_2Cl_2 solution was chromatographed on a silica gel column using Et_2O as the eluent. [Ac-Fc(4-py)] was isolated in 50% yield as a red powder from the second band. Anal. Calcd for $C_{17}H_{15}NOFe$: C, 66.91; H, 4.95; N, 4.59. Found: C, 66.80; H, 5.06; N, 4.50. ^{1}H NMR ($CDCl_3$): δ 8.68 (d, 2H), 7,30 (d, 2H), 4.65 (t, 2H), 4.53 (t, 2H), 4.36 (t, 2H), 4.27 (t, 2H), 2.05 (s, 3H). ^{13}C NMR-($CDCl_3$): δ 200.8, 149.2, 146.0, 121.2, 82.5, 80.3, 73.7, 71.6, 71.0, 68.0, 27.1.

Preparation of 1-Bromo-1′-(4-pyridyl)ferrocene, [Br-Fc(4-py)]. A 250 mL round-bottomed flask containing 100 mL of Et_2O, 16.6 mg (31 μmol) of *cis*-(1,3-bis(diphenylphosphino)propane)−dichloronickel and 300 mg of Mg was equipped with a magnetic stirring bar, condenser, and argon inlet and outlet. To this flask was slowly added 2.05 g (13 mmol) of 4-bromopyridine. The resulting mixture was stirred for 40 min. The reaction was quenched by slow addition of 20 mL of H_2O, and the ethereal layer was collected, dried over $MgSO_4$, and chromatographed on a silica gel column using Et_2O as the eluent. [Br−Fc(4-py)] was isolated in 5% yield from the third band as a red powder. Anal. Calcd for $C_{15}H_{12}NBrFe$: C, 52.68; H, 3.54; N, 4.10. Found: C, 52.41; H, 3.62; N, 4.01. ^{1}H NMR ($CDCl_3$): δ 8.56 (d, 2H), 7.36 (d, 2H), 4.69 (t, 2H), 4.45 (t, 2H), 4.13 (t, 2H), 3.97 (t, 2H). ^{13}C NMR ($CDCl_3$): δ 149.5, 146.8, 120.9, 82.7, 78.1, 72.5, 72, 69.2, 68.9.

Preparation of $[Et\text{-}Fc(4\text{-}py)Ru(NH_3)_5](PF_6)_2$. The same procedure[14] for the preparation of $[H-Fc(4\text{-}py)Ru(NH_3)_5](PF_6)_2$ was adopted here starting from $[Ru(NH_3)_5(OH_2)](PF_6)_2$ (100 mg, 0.21 mmol) and [Et-Fc(4-py)] (100 mg, 0.34 mmol). The purified product was an orange powder and weighed 120 mg (0.16 mmol). Anal. Calcd for $C_{17}H_{32}N_6P_2F_{12}FeRu$: C, 26.61; H, 4.20; N, 10.95. Found: C, 26.32; H, 4.30; N, 10.80. ^{1}H NMR (acetone-d_6): δ 8.63 (d, 2H), 7.43 (d, 2H), 4.88 (t, 2H), 4.46 (t, 2H), 3.96 (t, 2H), 3.92 (t, 2H), 3.05 (s, 3H), 2.58 (s, 12H), 2.22 (q, 2H), 1.07 (t, 3H).

Preparation of $[Br\text{-}Fc(4\text{-}py)Ru(NH_3)_5](PF_6)_2$. The same procedure was followed using $[Ru(NH_3)_5(OH_2)](PF_6)_2$ (100 mg, 0.21 mmol) and [Br−Fc(4-py)] (100 mg, 0.29 mmol). The purified product was an orange powder and weighed 150 mg (0.18 mmol). Anal. Calcd for $C_{15}H_{27}N_6BrP_2F_{12}FeRu$: C, 22.02; H, 3.33; N, 10.27. Found: C, 21.90; H, 3.43; N, 10.15. ^{1}H NMR (acetone-d_6): δ 8.66 (d, 2H), 7.46 (d, 2H), 4.95 (t, 2H), 4.57 (t, 2H), 4.29 (t, 2H), 4.09 (t, 2H), 3.07 (s, 3H), 2.58 (s, 12H).

Preparation of $[Ac\text{-}Fc(4\text{-}py)Ru(NH_3)_5](PF_6)_2$. The same procedure was followed using $[Ru(NH_3)_5(OH_2)](PF_6)_2$ (100 mg, 0.21 mmol) and [Ac−Fc(4-py)] (100 mg, 0.33 mmol). The purified product was an orange powder and weighed 130 mg (0.17 mmol). Anal. Calcd for $C_{17}H_{30}N_6OP_2F_{12}FeRu$: C, 26.13; H, 3.87; N, 10.76. Found: C, 25.92; H, 3.95; N, 10.60. ^{1}H NMR (acetone-d_6): δ 8.67 (d, 2H), 7.42 (d, 2H), 4.97 (t, 2H), 4.65 (t, 2H), 4.57 (t, 2H), 4.42 (t, 2H), 3.10 (s, 3H), 2.60 (s, 12H), 2.21 (s, 3H).

CV. Cyclic voltammetric experiments were carried out with the use of a Princeton Applied Research (PAR) Model 273 electrochemistry system and a standard three-electrode configuration. Cyclic voltammograms were recorded with a platinum working electrode (0.28 cm^2), a platinum wire, and a nonaqueous reference electrode (Ag/0.1 M $AgNO_3$ in CH_3CN) located inside a reference electrode bridge tube with a Vycor tip (PAR−K0065) to prevent contamination of the test solution by the reference electrode filling solution. The three electrodes were kept in situ, and the ferrocenium/ferrocene couple was used as

(35) Blackbourn, R. L.; Hupp, J. T. *J. Phys. Chem.* **1990**, *94*, 1788.
(36) Blackbourn, R. L.; Dong, Y.; Lyon, A.; Hupp, J. T. *Inorg. Chem.* **1994**, *33*, 4446.
(37) Brunschwig, B. S.; Sutin, N. *Coord. Chem. Rev.* **1999**, *187*, 233.
(38) Shriver, D. F.; Drezdon, M. A. *The Manipulation of Air-Sensitive Compounds*; John Wiley & Sons: New York, 1986.
(39) Perrin, D. D.; Armarego, W. L. F.; Perrin, D. R. *Purification of Laboratory* Chemicals, 2nd ed.; Pergamon Press: New York, 1980.
(40) Schechter, H.; Helling, J. F. *J. Org. Chem.* **1961**, *26*, 1034.
(41) Tamao, K.; Kodama, S.; Nakajima, I.; Kumada, M.; Minato, A.; Susuki, K. *Tetrahedron* **1982**, *38*, 3347.

an internal standard. Solutions were ca. 1.0×10^{-3} M in the complex and 0.1 M in $(Bu_4N)PF_6$ and purged with argon for 15 min prior to each measurement. The scan rates were 200 mV/s. The $E_{1/2}$ values were calculated from the average of the cathodic and anodic potentials.

Spectroscopic Studies. UV−vis and near-IR spectra were recorded at 298 ± 0.5 K with a Shimadu 3101 PC spectrophotometer equipped with a thermostatic cell holder. Experiments were carried out by mixing 1 mL each of the oxidant (2×10^{-3} M ferrocenium hexafluorophosphate) and the reductant (ca. 1×10^{-3} M complex) prepared solutions for near-IR measurements in a side-armed flask containing the solvents chosen. The reactions were controlled at 298 ± 0.5 K for 2 h. The resulting solution was then transferred to a 1 cm matched quartz cell capped with a septum using the syringe technique. Intervalence charge transfer spectra were recorded and analyzed with ORIGIN, a Gaussian fitting program.[42]

Acknowledgment. We gratefully acknowledge support from the National Science Council (Grant NSC-86-2113-M-030-008). Partial support of this research by a Grant-in-Aid for Scientific Research of the SVD Section, Fu Jen University, is also greatly appreciated.

IC990839J

(42) Gaussian fittings were carried out for near-IR spectra employing release 4.0 of ORIGIN, MICROCAL Software, Inc., Northampton, MA 01060.